International Journal of Research Publication and Reviews, Vol 6, Issue 6, pp 905-919 June 2025

International Journal of Research Publication and Reviews

Journal homepage: www.ijrpr.com ISSN 2582-7421

Rock Mass Characterization and Kinematic Stability Analysis of the Chingola Open Pit F and D (COP F&D), Nchanga Mine, Zambia

Nickson Lushasi [a*], *Bunda Besa* [b], *Donald Chishimba* [c]

[a] *Postgraduate Student, University of Zambia, School of Mines, Department of Mining Engineering, P.O Box 32379, Lusaka, Zambia*
[b] *University of Zambia, School of Mines, Department of Mining Engineering, P.O Box 32379, Lusaka, Zambia*
[c] *Head Geotechnical-KIBU-Technical Services, Konkola Copper Mines Plc, Chililabombwe, Zambia*

A B S T R A C T

The Chingola Open Pit F and D (COP F&D) area has a complex geology characterized by varying degrees of mechanical strength and a history of slope failures. This study aimed to conduct a rock mass characterization based on lithological distribution and assess the kinematic feasibility of the COP F&D pit. Additionally, to evaluate the extent of variation among different lithological strength parameters.

Utilizing data from borehole logging, field-based discontinuity mapping, and laboratory testing, the Rock Mass Rating (RMR) and Geological Strength Index (GSI) systems were applied to evaluate rock quality. Stereographic analysis was performed using DIPS software to assess the potential for various slope failure modes in the study area.

The study characterized 13 distinct lithologies in the area, which exhibited fair to poor quality, classified as RMR Classes III and IV. In contrast, the basement rock formation (BAS) demonstrated better mechanical competence and was classified as Class II, with an overall average RMR of 63 and a GSI of 58. Qualitatively, the basement rock formation is characterized as good rock, composed of multi-faceted angular block structures with three or more joint sets. The results also indicated significant variability in lithological strength parameters, with a coefficient of variation exceeding 30%. The kinematic analysis results were validated using the criteria proposed by Norrish and Wyllie (1992), which indicated susceptibility to planar, wedge, and toppling failures.

In conclusion, the study found that the area has variable lithological strength parameters and adversely oriented discontinuities that pose a risk for slope failures. This variability indicates significant heterogeneity in rock mass properties, contributing to greater uncertainty in stability assessments, highlighting the need for enhanced geotechnical assessment and slope management.

Keywords: ***Rock mass characterization, Kinematic analysis, Rock lithology, Failure modes, Slope stability***

1. Introduction

The stability of mine excavations is of critical concern in the mining industry, as it directly impacts workers' safety and the economic viability of mining operations (Kolapo et al., 2022; Chishimba & Besa, 2023). Modern open-pit mines are often designed to extract resources from steeper and higher slopes, which makes them more susceptible to slope failures (Kolapo et al., 2022; Obregon & Mitri, 2019; Verma et al., 2011). To ensure the safety of mine sites, rock slope stability assessment is crucial for both designing and continued evaluation of rock slopes (Ahmed et al., 2018; Dzimunya et al., 2023; Bieniawski, 1989; Woldeselsassie et al., 2019). Slope instability in open-pit mines arises from a combination of geotechnical, geological, and external factors. These include the inherent strength properties of the rock mass, groundwater conditions, orientation and condition of discontinuities, and external influences such as rainfall and blasting activities (Abramson et al., 2002; Woldeselsassie et al., 2019). Natural slopes that have remained stable over long periods may experience sudden failures as a result of alterations in slope geometry, reduction in shear strength, or the influence of external forces (Abramson et al., 2002). Notably, the spatial variability in geomechanical properties across various lithological units induces uncertainty in evaluating the slope behaviour and compromises the optimal design of pit slopes (Rafiei Renani et al., 2019; Aladejare & Akeju, 2020).

To address these challenges, empirical rock mass classification systems, such as the Rock Mass Rating (RMR), Geological Strength Index (GSI), and Slope Mass Rating (SMR), have become essential tools in geotechnical analysis. These empirical systems provide a structured approach in characterizing rock masses and predicting their mechanical behaviour. Complementing these, kinematic stability analysis using stereographic projections has proven effective in identifying structurally controlled failure modes such as planar, wedge, and toppling failures (Hoek & Bray, 1981; Verma et al., 2021).

The study area, COP F&D, is a compelling case for assessing slope stability because of its geological complexity and history of slope failures. It contains a diverse range of lithologies, each with different mechanical strengths, yet there has been limited research on how these variations affect slope stability.

This study aims to address this gap by performing a comprehensive rock mass characterization based on lithological distribution, along with a kinematic stability assessment of the COP F&D pit. The study evaluates the extent of variability in strength parameters across different lithologies.

2.0 Rock Mass Classification and Kinematic Stability Analysis

2.1 Rockmass Classification Schemes

Different scholars have put forth various classification schemes for rock masses, which have a wide range of uses in different aspects of rock mechanics (Bieniawski,1989; Deere et al.,1967; Romana, 1985; Laubscher, 1990; Hoek et al., 1994). Bieniawski (1973) introduced the RMR system, which has undergone significant modifications to the ratings assigned for different parameters due to continued research. It is now widely used in the mining and geotechnical engineering fields for rockmass characterization and classification purposes (Bieniawski, 1989). To characterize a rock mass, the RMR system uses six parameters, the values of which are added to produce the overall RMR rating, as expressed in Equation 1.

$$RMR = RQD_r + UCS_r + J_{c_r} + J_{s_r} + G_{w_r} + J_{\vartheta_r} \quad (1)$$

Where; RQD_r stands for the Rock Quality Designation rating; J_{s_r} is the rating for joint/discontinuity spacing; J_{c_r} is the rating for condition of discontinuities; G_{w_r} is the rating for groundwater condition; UCS_r is rating for the uniaxial compressive strength of intact rock, and J_{ϑ_r} represents the rating for orientation of discontinuities.

The Rock Quality Designation Index (RQD) was developed by Deere et al., (1967) as a means to quantitatively estimate the rock mass quality from drill core logs. It represents an adjusted percentage of core recovery, considering only unbroken core segments that are at least 10 cm long along the core axis, as defined by Equation 2 (Singh & Goel, 2011).

$$RQD = \frac{Sum\ of\ core\ pieces \geq 10cm}{Total\ Core\ run} \times 100\% \quad (2)$$

In situations where there is limited availability or no cores available at all, the RQD may simply be determined from the 'Volumetric Joint Count' method as introduced by Palmstrom in 1982 using the following correlation as expressed in Equation 3 (Singh & Goel, 2011);

$$RQD = 115 - 3.3J_v \quad (3)$$

Where; J_v represents the total number of joints per cubic meter, commonly known as the volumetric joint count.

The Slope Mass Rating (SMR) system as a modification to the Bieniawski's (1974) RMR was proposed by Romana (1985) and it's a very useful tool for assessing the slope risk and stability of rock slopes. The use of SMR provides a quick assessment about the slope behaviour at any point and it is one of the most accepted, versatile and widely used tool in surface mines (Verma et al., 2011). It is mathematically represented by Equation 4 (Singh et al., 2011);

$$SMR = RMR_{basic} - (F_1.F_2.F_3) + F_4 \quad (4)$$

Where; RMR_{basic} is the Rock Mass Rating evaluated without considering the orientation of discontinuities; F_1, F_2, and F_3 are adjustment factors that account for the orientation of joints relative to the slope orientation; and F_4 is the correction factor which depends on the method of excavation. Five stability classes were defined by Romana (1985) based on SMR values as described in Table 1.

Table 1: Stability Classes based on SMR Values (Romana, 1985)

1. **Class**	2. **V**	3. **IV**	4. **III**	5. **II**	6. **I**
7. **SMR Values**	8. 0-20	9. 21-40	10. 41-60	11. 61-80	12. 81-100
13. **Rockmass description**	14. Very bad	15. Bad	16. Normal	17. Good	18. Very good
19. **Stability**	20. Completely unstable	21. Unstable	22. Partially stable	23. Stable	24. Completely stable
25. **Possible Failures**	26. Big planar or soil-like or circular failure	27. Planar or big wedges	28. Planar along certain joints and many wedge failure	29. Some block failure	30. No failure
31. **Probability of failure**	32. 0.9	33. 0.6	34. 0.4	35. 0.2	36. 0

Laubscher made several modifications to the Bieniawski's RMR system to better suit mining applications over the years (Laubscher and Taylor, 1976; Laubscher, 1977, 1984; and Laubscher and Page, 1990). These modifications culminated in the development of the Mining Rock Mass Rating (MRMR) system in 1990 (Laubscher, 1990). The MRMR system is extensively used in mining to assess the stability and quality of rock masses and it takes into account similar parameters as applied to the Bieniawski's RMR (Simataa, 2019). However, the MRMR takes additional factors into consideration, including excavation techniques, stress effects, discontinuity orientation, and potential future weathering. This makes it to be more tailored to mining applications, providing a more comprehensive assessment of rock mass stability and support requirements. Mathematically, it may be expressed as in Equation 5;

$$MRMR = RMR^{*} \times Adjustment\ factors \quad (5)$$

Where; RMR^{*} is the Laubscher's Rock mass Rating which is dependent on four parameters, as defined by Equation 6;

$$RMR^{*} = RQD + IRS + J_s + J_c^{*} \quad (6)$$

Where; IRS is the Intact Rock Strength rating, J_s indicates the rating for spacing of discontinuities, and J_c^{*} represents the rating for condition of discontinuities which is dependent on presence of groundwater and pressure or quantity of groundwater inflow in the underground excavation.

Barton et al. (1974) developed the Q-system to evaluate the rock mass quality, aiding in the preliminary empirical design of support structures for tunnels and caverns. As noted by Singh & Goel (2011), it is a quantitative classification system used to estimate tunnel support, based on evaluation of the rock mass quality using six defined parameters. The six parameters are: Rock Quality Designation (RQD); Number of joint sets (J_n); Joint roughness number for the critically oriented joint set (J_r); Degree of alteration or filling along the weakest/critically oriented joint set (J_a); Water inflow or joint water reduction factor (J_w); and Stress condition given as the stress reduction factor (SRF). The rockmass quality (Q) is empirically defined using the following relationship;

$$Q = \left[\frac{RQD}{J_n}\right] \cdot \left[\frac{J_r}{J_a}\right] \cdot \left[\frac{J_w}{SRF}\right] \quad (7)$$

Hoek (1994) developed the Geological Strength Index (GSI) as an alternative for characterising the rock mass quality, aiming to overcome the difficulties associated with applying Bieniawski's (1978) RMR to extremely poor rock masses. It was introduced as a method for collecting field data to estimate the rock mass constants $m_i, s,$ and a in the generalized Hoek-Brown failure criterion. GSI was also designed to address rock masses composed of interlocking angular blocks, where failure primarily occurs through block sliding and rotation rather than intact rock failure (Hoek & Brown, 2019). Furthermore, GSI is an important tool for estimating parameters such as cohesion, friction angle and deformation modulus of rock masses (Ndlovu & Louis Van Rooy, (2018). The GSI chart introduced by Hoek & Brown (1997) aids in initial rock mass property estimation, with the expectation that users refine these estimates through further site investigations and analyses (Hoek & Brown, 2019). The GSI chart was developed based on the following correlations, expressed in Equations 8 and 9 (Singh & Goel, 2011);

$$GSI = RMR_{89} - 5; \quad \text{for } GSI \geq 18 \ or \ RMR \geq 23; \quad (8)$$

$$GSI = 9lnQ' + 44\ ; \quad \text{for } GSI < 18 \ or \ RMR < 23 \quad (9)$$

Where; RMR_{89} is the rockmass rating according to Bieniawski (1989), and Q' is the modified rockmass quality, defined by Equation 10;

$$Q' = \left(\frac{RQD}{J_n}\right) \cdot \left(\frac{J_r}{J_a}\right) \quad (10)$$

In a nutshell, when applied correctly, rock mass classification systems serve as an effective design tool and can sometimes be the sole practical foundation for the design (Dyke, 2008).

2.2 Kinematic Stability Analysis

Kinematic analysis is one of the conventional methods of slope stability analysis developed by Markland (1972), and later modified by Hocking (1976) and Hoek & Bray (1981), as cited from Awang et al., (2021) and Salmanfarsi et al., (2020). It has been in use for several decades and uses stereonets to predict the risks of failure in rock slopes (Awang et al., 2021; Hoek & Bray, 1981; Salmanfarsi et al., 2020). It is based on the geometrical relationship of the discontinuities present in a slope mass and provides information not only about the mode of failure but also takes into account the friction angle and cohesion, and also helps to predict the factor of safety or probability of failure of rock slopes (Verma et al., 2021).

Sandria et al., (2023) used stereographic projection to predict the risk of failure at both the inlet and outlet portals of the diversion tunnel. Analysis results indicated the risk of both flexural and oblique toppling failures at both portals, whereby validation of results was done against conditions necessary for planar, wedge, and toppling failures (Sandria et al., 2023). Kinematic analysis involves assessing the orientation of discontinuity sets and the slope face, along with friction, to identify possible failure modes (Awang et al., 2021). Kinematic analysis has been commonly used for local slope stability analyses, either independently or in conjunction with other methods. Over the years, kinematic analysis and rock mass classification have have consistently demonstrated their reliability and efficacy in evaluating the stability of rock slopes. These methods remain extensively adopted in Malaysia and are well-accepted in the fields of engineering geology and geotechnical engineering (Salmanfarsi et al., 2020). Kinematic analysis, however, is only applicable to structurally controlled cut slopes and tends to ignore the strength parameters of the discontinuities and rock mass, as well as the forces acting on the slope (Alzo'ubi, 2016). Despite its limitations, it continues to play a vital role in assessing structurally controlled rock slopes and is advised as the first step before employing other slope stability analysis methods (Raghuvanshi, 2019; Salmanfarsi et al., 2020).

2.3 Slope Stability Monitoring

Once the initial stability assessment is completed, ongoing monitoring is crucial to detect any changes that may indicate instability or failure of the slope. Stability assessments and monitoring can be achieved via a number of methods from detailed geotechnical field investigation and using monitoring techniques which include both field observations/visual surveys, prism monitoring, and advanced methods like Laser scanning (LiDAR) and Slope Stability Radar (SSR) (Mohammed, 2021). Geotechnical engineers are advised to incorporate the SSR as a robust and powerful tool for slope design and analysis since it can reveal critical behaviors that might otherwise remain undetected (Salunke et al., 2017). However, each technique offers unique benefits; hence, a combination of more than one technique provides a more comprehensive monitoring of pit slope stability in an area (Oosthuizen, 2018; Srinivasan et al., 2016).

The SSR technology has been commonly used at the study area (COP F&D) to monitor slope movements as shown by Figure 1;

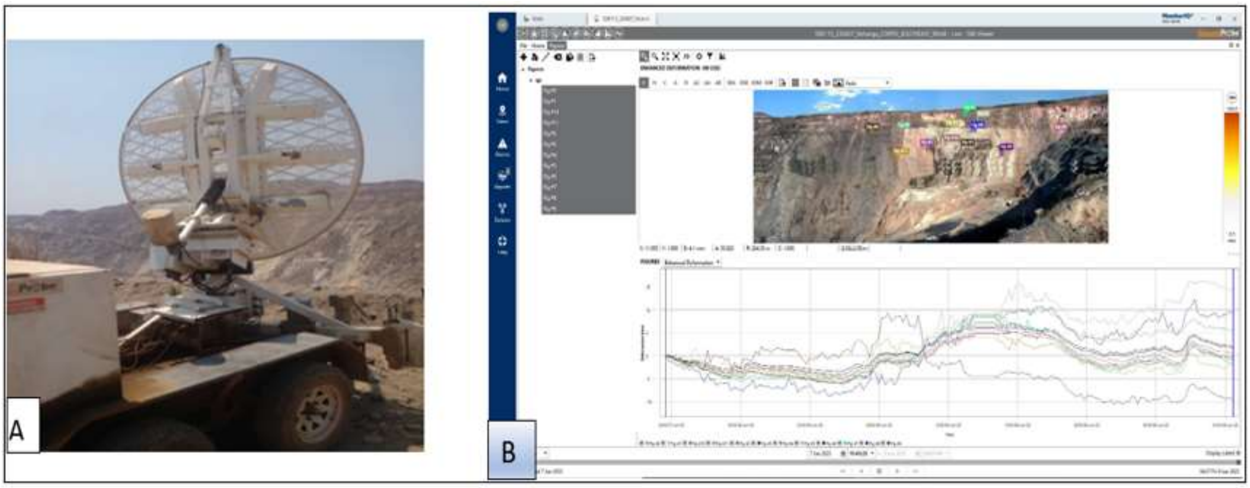

Figure 1: Slope stability monitoring at COP F&D using SSR; (A)-SSR monitoring the East wall; (B)- Deformation plot and graph of instability

3.0 Methodology

The study involved a detailed geological and geotechnical field investigation (mapping), core logging and laboratory tests. The rock mass was classified while taking into account all related lithologies, using Bieniawski's (1989) RMR system and the Hoek-Brown GSI. Data from 23 logged boreholes was used to evaluate the rock mass characterization.

The basic RMR was calculated based on five parameters: Rock Quality Designation (RQD), Unconfined Compressive Strength (UCS) of intact rock, conditions of discontinuities, spacing between discontinuities, and groundwater condition. The RQD was estimated based on borehole data using Equation 2. The UCS was obtained from laboratory tests, while other parameters were measured from the field. A kinematic feasibility analysis of the study area was conducted using Rocscience software (Dips version 6.008) to identify potential failure modes based on mapped discontinuity data. Figure 2 shows the author conducting the discontinuity mapping process in the field.

Figure 2: Field discontinuity mapping at the study area

3.1 Description and location of the study area

The study was conducted at COP F&D, which forms part of the Nchanga Open Pit (NOP) mine. This mine is located in Chingola town on the Zambian Copperbelt, approximately 420 kilometres from Lusaka, the capital city of Zambia. NOP mine started its mining operations in 1938 and is currently owned and operated by the Konkola Copper Mines (KCM) PLC which is an integrated copper producer operating on the Copperbelt in Zambia. Covering nearly 35 km², it is one of the largest open pit mines in the world, with the deepest part of the pit being over 400m lower than the surrounding plateau (Gong et al., 2021). Rope shovels, hydraulic shovels and haul trucks operated by KCM and contractors are used for excavation and haulage of ore and waste in the pits. This study focused on COP F&D, which is one of the most productive and potential pits at the Nchanga Mine. The geological setting of the study area is shown in Figure 3.

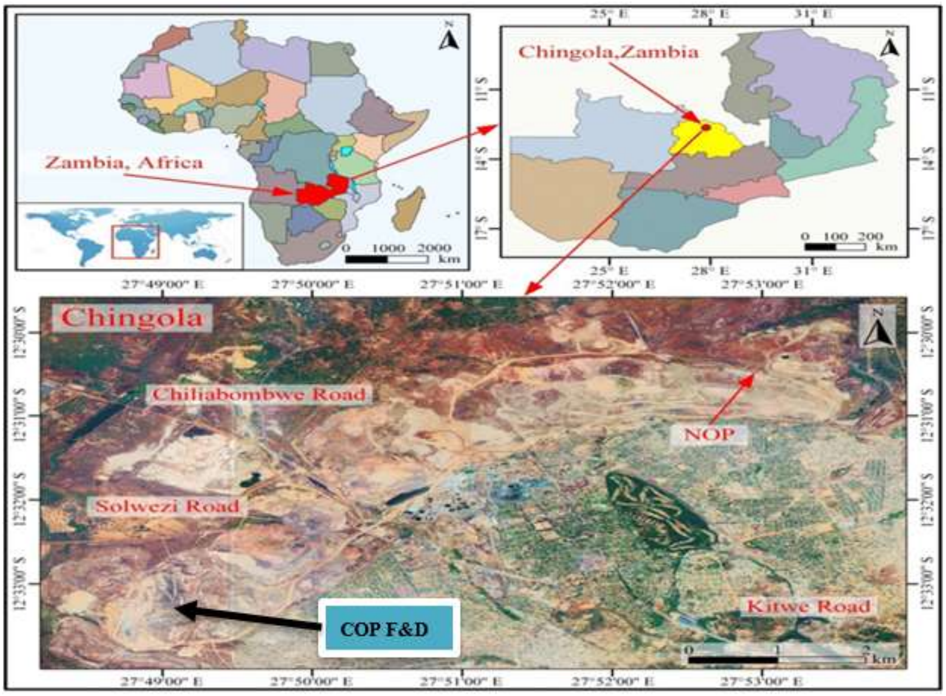

Figure 3: Geological location of the study area (Modified from Gong et al., 2021)

The study area is characterized by a variety of rock lithologies ranging from laterite to basement rock formations. The main rock layers and hydrogeological units in the study area are summarized in Table 2.

Table 2: The stratigraphy of COP F&D (Source: NOP Geology section)

37. Stratigraphy	**38. Thickness (m)**	**39. Hydrogeological Unit**
40. Upper Roan Dolomite (URD)	41. >400	42. Aquifer
43. Shale with Grit (SWG)	44. 70	45. Aquiclude
46. Chingola dolomite (CDOL)	47. 15	48. Aquifer
49. Dolomitic Schist (DOLSCH)	50. 20	51. Minor aquifer
52. Upper Banded Shale (UBS)	53. 18	54. Aquiclude
55. Feldspathic Quartzite (TFQ)	56. 18	57. Aquiclude
58. Banded Sandstone Upper (BSSU)	59. 15	60. Aquifer
61. Pink Quartzite (PQ)	62. 5	63. Aquiclude
64. Banded Sandstone Lower (BSSL)	65. 10	66. Aquifer
67. Lower banded shale (LBS)	68. 10	69. Aquiclude
70. Arkose (ARK), [Orebody]	71. 15	72. Minor aquifer
73. Basement Schist (BAS)	74. >400	75. Impermeable

4.0 Results and Discussion

4.1 Determination of the variability between rock mass strength parameters

The mean, standard deviation (S.D), and coefficient of variation (COV) for the intact rock UCS, tensile strength (σ_t), unit weight (Ɣ), cohesion (C), and friction angle (φ) were determined based on the different lithologies in the study area to account for their variability. The relationship between UCS and σ_t derivatives per rock lithology is presented in Figure 4.

Figure 4: Relationship between mean, standard deviation (S.D) and coefficient of variation (COV): **A**- Rock UCS; **B**- Rock tensile strength

From Figure 4, Dolomitic schist (DOLSCH) demonstrates both the lowest mean UCS and tensile strength (20MPa & 1.257 MPa respectively), while unveiling the highest variability respectively (66.4% & 81.3%). This indicates that this type of rock is more affected by weathering or is highly jointed, which corresponds with the observed site conditions.

The variability between selected rock parameters per lithology was assessed by computing their respective coefficients of variation. Very high COV values (>30%) are observed and this implies that the rockmass is mechanically weak and highly inconsistent in strength, which may have vital implications in engineering and geological context. From Figure 5, the cohesion (C) portrayed the highest COV (%) on average among all assessed parameters, with its lowest value (48.9%) being observed from TFQ and highest value (97.4%) from CDOL. The UCS and tensile strength (σ_t) also showed higher variability (>30%) on average across all lithologies, while the friction angle (φ) had moderate variability. Conversely, the unit weight (Ɣ) exhibited low variability (≈10%) across all lithologies as shown in Figure 5. This low variability in unit weight infers that the rocks in the area have a relatively uniform unit weight, which could benefit engineering and geological applications by simplifying calculations and stability predictions. The variability between selected parameters per lithology is graphically presented in Figure 5.

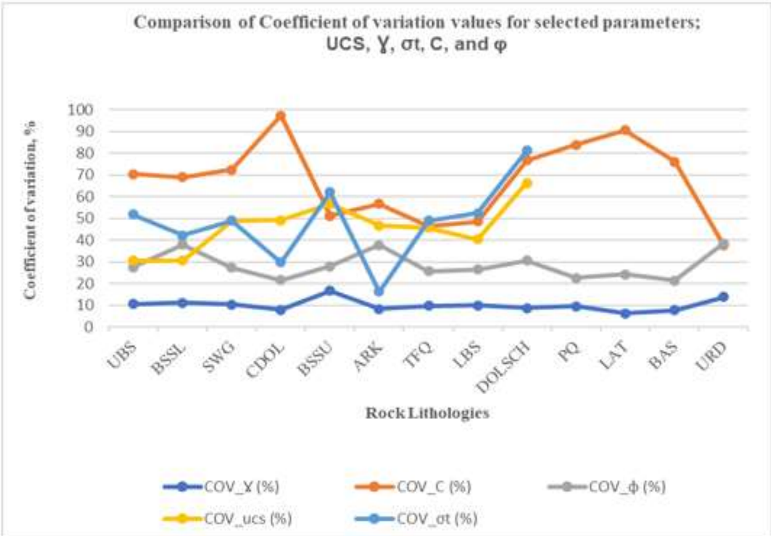

Figure 5: Comparison of lithological variability (%) across selected strength parameters

4.2 Rockmass Quality and Characterization Results

The rockmass quality and classification was performed based on data from 23 logged boreholes, laboratory tests, and field discontinuity mapping. The average RMR values of the contained lithologies from the selected logged boreholes varied significantly, ranging from 15 for laterite to above 70 for some arkose and basement rocks as indicated in Figure 6.

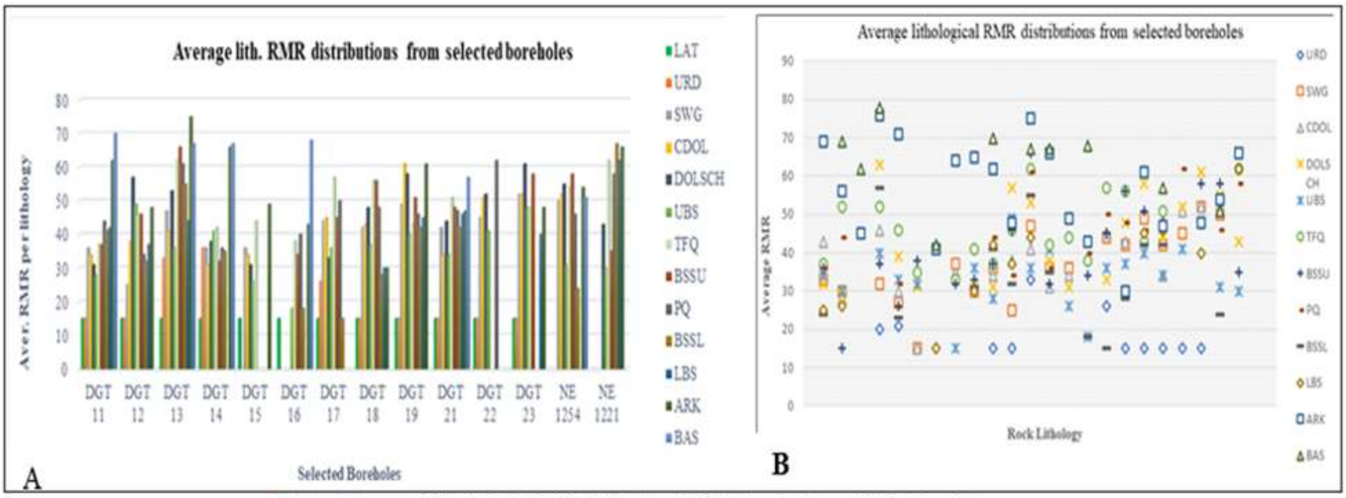

Figure 6: Average lithological RMR distribution: A-Clustered column; B- Scatter plot

The overall RMR and GSI values per lithology in the study area were computed from the mean lithological RMR values per borehole, based on data from 23 logged boreholes. These values, along with the rock quality description, are presented in Table 3.

Table 3: Overall average lithological RMR values, GSI values and Rock quality description

76. Lithology	77. Overall Average RMR	78. RMR Class	79. GSI	80. Quality Description
81. LAT	82. 15	83. V	84. -	85. Very poor rock
86. URD	87. 22	88. IV	89. -	90. Poor rock
91. SWG	92. 38	93. IV	94. 33	95. Poor rock
96. CDOL	97. 38	98. IV	99. 33	100. Poor rock
101. DOLSCH	102. 42	103. III	104. 37	105. Fair rock
106. UBS	107. 34	108. IV	109. 29	110. Poor rock
111. TFQ	112. 47	113. III	114. 42	115. Fair rock
116. BSSU	117. 41	118. III	119. 36	120. Fair rock
121. PQ	122. 47	123. III	124. 42	125. Fair rock
126. BSSL	127. 36	128. IV	129. 31	130. Poor rock
131. LBS	132. 37	133. IV	134. 32	135. Poor rock
136. ARK	137. 57	138. III	139. 52	140. Fair rock
141. BAS	142. 63	143. II	144. 58	145. Good rock

The overall average RMR and GSI values shown in Table 3 are graphically represented in Figure 7.

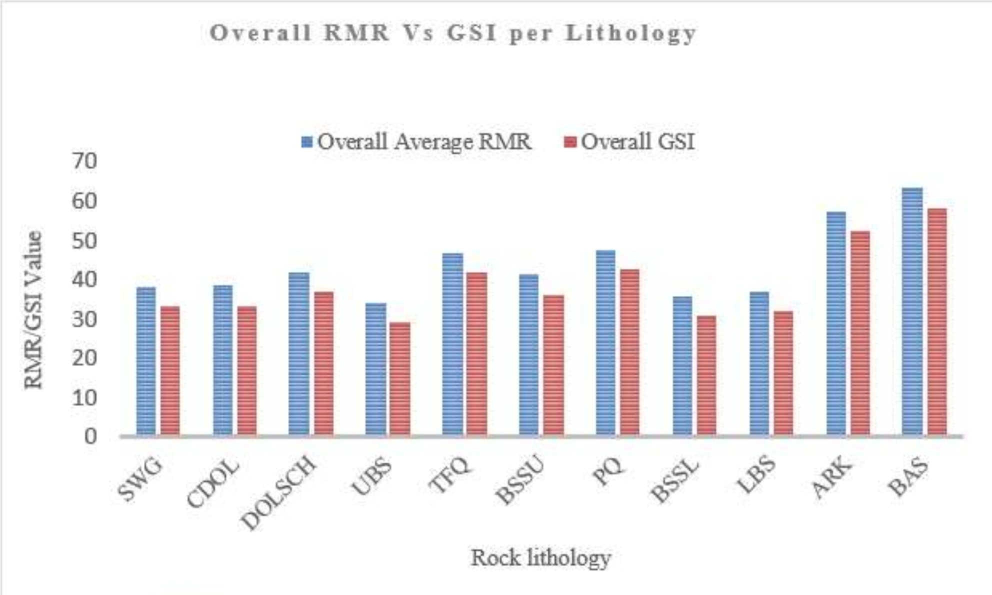

Figure 7: Overall mean RMR vs GSI per lithology around the study area

As depicted in Figure 7 and Table 3, most RMR/GSI values fall under classes III and IV, indicating fair and poor rock masses, respectively. However, the basement rock formation indicates a good quality rock mass (Class II) with an RMR value of 63. Similarly, a significant variation in GSI across all lithologies was observed, with the basement rock formation exhibiting the highest overall value of approximately 58. This highlights the need to prioritize the slope factor of safety when designing slope angles relative to slope heights, given the significant variation and scatter in the strength parameters (Figure 5) and rock mass rating values.

4.3 Determination of RMR standard deviation ($RMR_{\_S.D}$) and Coefficient of Variation

The standard deviation values ($RMR_{\_S.D}$) and coefficients of variation (COV) based on RMR for dominant rock lithological units around COP F&D were determined using Equations 11 and 12 respectively.

$$RMR_{\_S.D} = \sqrt{\frac{1}{n_s}\sum_{i=1}^{n_s}(d_i - m)^2} \tag{11}$$

$$COV,\% = \frac{\delta}{m} * 100\% \tag{12}$$

Where; d_i is the set of rock property data, m is the rock property mean, and n_s is the total number of available rock data. ‘Rock property data’ stands for RMR value over certain depth interval.

A significant scatter in the RMR standard deviation values relative to the mean was observed across different lithologies within COP F&D, with most values ranging between 8 and 14, as shown in Table 4. The RMR coefficient of variation (COV) for different lithologies was found to be consistently high, with all values exceeding 10% (Figure 8). This suggests significant variability and inconsistency in rockmass properties across different rock units within the pit, leading to unpredictable behavior and greater uncertainty in stability assessments, hence requiring more detailed investigations. For rock properties, a coefficient of variation of less than 10% is often considered good as it shows low variability and high reliability (ISSMGE-TC304, 2021). BSSL exhibited the highest RMR coefficient of variation, approximately 41%, while BAS showed the lowest value at 16.6% (Table 4).

Table 4: RMR Standard deviation and Coefficient of variation

146. Lithology	**147. Average RMR**	**148. STD DEV**	**149. COV (%)**
150. LAT	151. 15	152. 0	153. 0
154. URD	155. 22	156. 8.443	157. 38.1
158. SWG	159. 38	160. 9.76	161. 25.4
162. CDOL	163. 38	164. 11.475	165. 29.9
166. DOLSCH	167. 42	168. 12.692	169. 30.4
170. UBS	171. 34	172. 8.092	173. 23.8
174. TFQ	175. 47	176. 8.532	177. 18.2
178. BSSU	179. 41	180. 12.346	181. 30

182. PQ	183. 47	184. 11.294	185. 23.8
186. BSSL	187. 36	188. 14.579	189. 41
190. LBS	191. 37	192. 11.902	193. 32.3
194. ARK	195. 57	196. 12.265	197. 21.4
198. BAS	199. 63	200. 10.477	201. 16.6

Graphically, the relationship between the calculated standard deviation and coefficient of variation is presented in Figure 8;

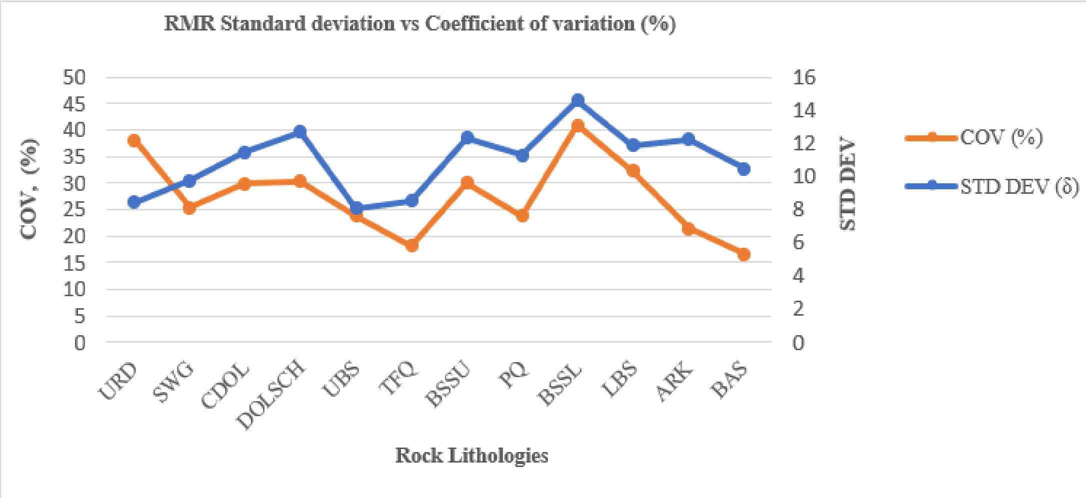

Figure 8: Relationship between RMR Standard Deviation and Coefficient of variation (%)

4.4 Kinematic feasibility analysis for the study area

Different values for the discontinuity dip/dip direction and slope face angles at prospective pit benches were determined via window mapping at several locations. The analysis was performed using DIPS software, employing stereonets to determine various failure modes at different depths for the southern and western walls of COP F&D. Analysis results revealed presence of up to three clusters of joints, with varying maximum density. Table 5 shows the dip and dip direction of mean discontinuity planes from the assessed locations.

Table 5: Dip and dip direction of mean discontinuity set planes from assessed locations.

Location ID	Joint set #	Dip (º)	Dip Direction (º)	Location ID	Joint set #	Dip (º)	Dip Direction (º)
L1	J1	44	312	**L5**	J1	36	258
Slope dip: 50º	J2	71	329	Slope dip: 65º	J2	66	098
Slope dip dir: 347	J3	83	243	Slope dip dir: 075			
L2	J1	62	098	**L6**	J1	80	097
Slope dip: 72º	J2	51	043	Slope dip: 76º	J2	86	009
Slope dip dir: 122	J3	63	198	Slope dip dir: 056	J3	90	176
L3				**L7**			
Slope dip: 67º	J1	98	051	Slope dip: 44º	J1	44	267
Slope dip dir: 078				Slope dip dir: 276			
L4	J1	48	291				
Slope dip: 55º	J2	47	090				
Slope dip dir: 020							

The analysis was done based on seven different feasible locations for all failure modes, with only the representative key findings illustrated in Figures 9-11 under the current study.

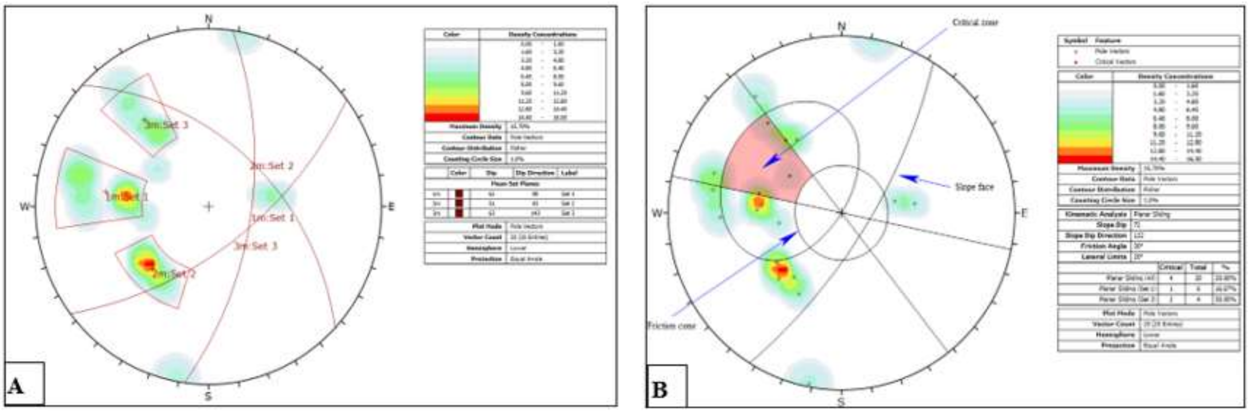

Figure 9: Kinematic analysis for location 2; (A)-Clusters of major joint sets, (B)- Planar failure analysis

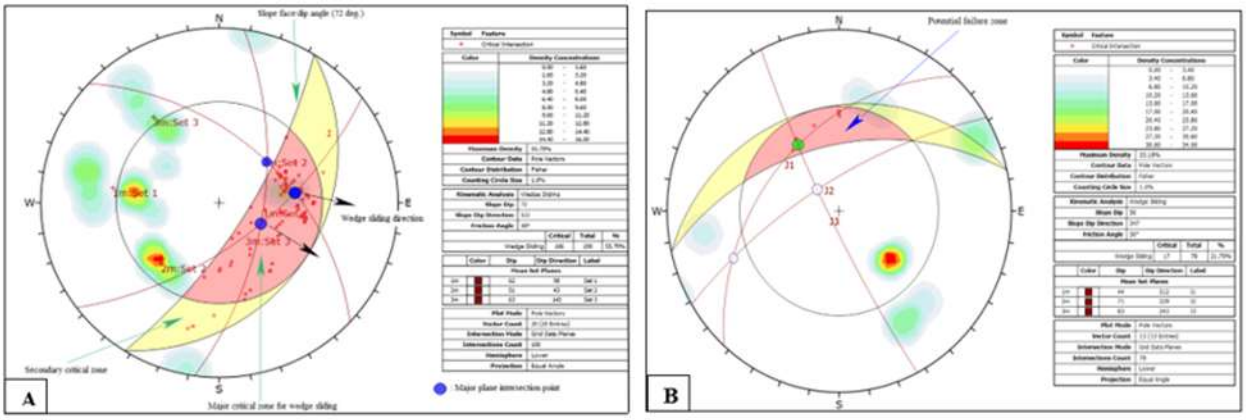

Figure 10: Wedge failure analysis: (A)-Location 2; (B)-Location 1

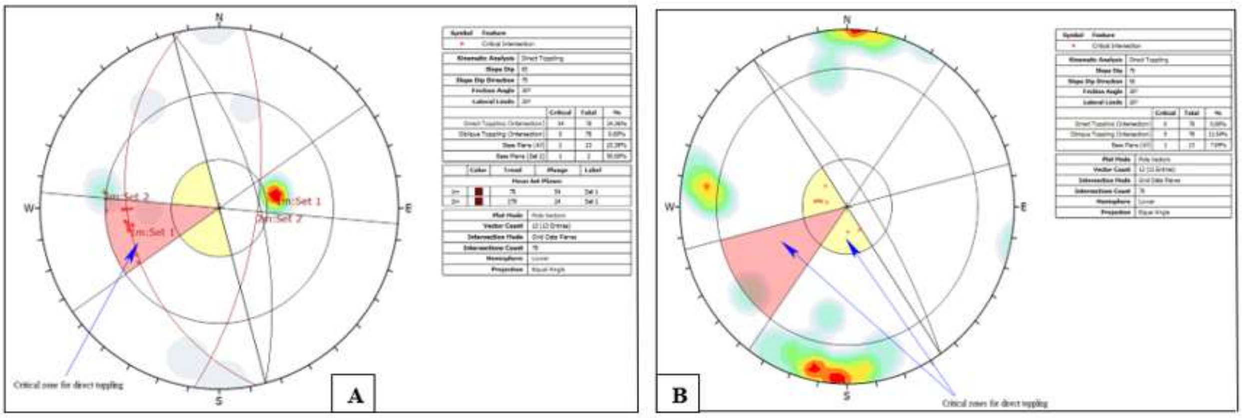

Figure 11: Toppling failure analysis: (A)-Direct toppling at location 5; (B)-Direct toppling at location 6

A summary of failure probabilities from all assessed areas is presented in Table 6.

Table 6**:** Summarized failure types and failure probabilities for all assessed locations

Location ID	Planar failure (Overall) (%)	Wedge failure (%)	Toppling failure (%)			
			Direct	Flexural	Oblique	Base plane (All)
Location 1	7.69	21.79	8.97	0.00	1.28	0.00
Location 2	20	55.79	1.05	0.00	0.00	20
Location 3	0.00	0.00	41.56	0.00	0.00	0.00
Location 4	0.00	10.26	0.00	7.69	1.28	0.00

Location 5	7.69	14.10	24.36	0.00	0.00	15.38
Location 6	15.38	37.18	0.00	0.00	11.54	7.69
Location 7	38.46	29.49	0.00	0.00	0.00	53.85

The failure probabilities presented in Table 6 are graphically depicted in Figure 12 as indicated.

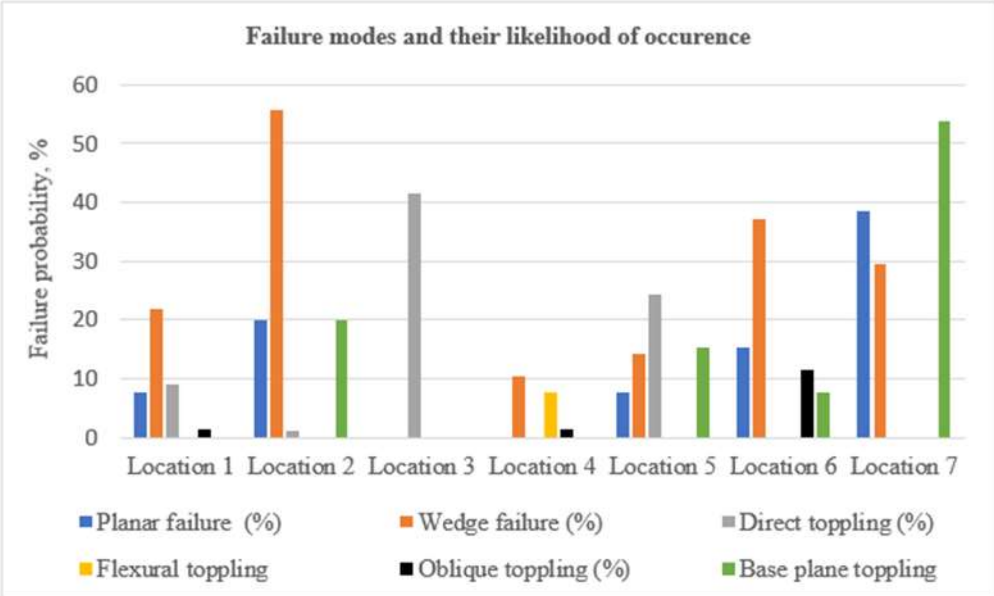

Figure 12: Failure modes and their likelihood of occurrence from assessed locations

4.5 Interpretation of Kinematic Analysis Findings

The general rule of thumb requires that any contour plot characterized by clusters of joints having a maximum density of greater than 15% should be handled carefully. All of the sites where the investigations were carried out had higher density concentrations exceeding 15%. This highlights the need for extra attention on these areas during stability assessments, as they may experience unexpected failures. The conducted analysis illustrates the following findings:

Based on Figure 12, the assessed areas are highly prone to wedge, planar, and toppling failures as detailed below:

- For wedge slope failures, location 2 showed the highest probability of wedge sliding at 55.79%, followed by location 6 with a wedge failure probability of 37.18%, and location 7 with a failure probability of 29.49%. Similarly, location 1 had a wedge sliding probability of 21.79%, while location 5 demonstrated a failure probability of 14.10%, and location 4 had a lower potential for wedge sliding at 10.26%.
- For planar failures, location 7 showed the highest probability of planar sliding at 38.46%, followed by location 2 with a 20.00% failure probability and location 6 with a 15.38% risk of planar sliding. Locations 1 and 5 exhibited low risks for planar sliding, each about 7.69%, while locations 3 and 4 did not show any potential for planar failures at the assessed slope orientations.
- The assessment of toppling failures across the seven locations indicated varying likelihoods of occurrence. Location 3 had the highest rate of direct toppling failure at 41.56%, while Location 7 indicated a very high overall probability of 'base plane' toppling failure at 53.85%. Location 5 showed high direct toppling failure rates of 50% from joint set 2 and 24.36% overall. At Location 2, the probability of 'base plane' direct toppling failure was 20%. Location 6 demonstrated potential for 'oblique toppling' with a probability of 11.54%. Location 1 showed a direct toppling failure rate of 8.97%, and Location 4 displayed probabilities for flexural toppling at 7.69% and 'oblique toppling' at 1.28%.

The analysis implies that more detailed investigations and intensive analysis using advanced approaches should be conducted around the study area to authenticate the results. This is in accordance to the suggestions by Rocscience, (2024) that results from kinematic analysis should always be accompanied by detailed field investigations and analysis techniques involving factor of safety calculations in places where risks of failure have been identified.

Rocscience (2024) states that while kinematic analysis can show potential risks for failure, it does not guarantee that a failure will happen. This is due to the fact that there are factors other than kinematics and friction such as joint cohesion and persistence which may come together to increase stability. Nonetheless, it should be noted that the stability of a slope, which may appear kinematically safe from failures, can suddenly be compromised by factors such as water pressure. This underscores the need for continuous slope stability monitoring in all areas, regardless of their current status.

4.6 Validation of Kinematic Analysis Results

The results from kinematic analysis for the assessed locations were validated against some simplified conditions for occurrence of planar, wedge, and toppling failures as described by Norrish & Wyllie, (1992). Table 7 shows the justification of simplified necessary conditions and reasons for occurrence of each failure.

Table 7: Justification for failure probability in accordance to the required conditions

Location ID	**Failure mode**	**Possibility of occurrence**	**Reason (s)**
L1	Planar	√	• Dip of the sliding plane is greater than the friction angle, i.e. $44^{o} > 30^{o}$ • The sliding plane daylights on the slope face, i.e. Dip of sliding plane < slope face angle ($44^{o} < 50^{o}$)
	Wedge	√	• There was intersection of two discontinuity planes, J_1 &J_3 within the failure zone • The slope geometry was steep enough to allow the wedge to slide out under gravity, i.e. 50^{o}
	Toppling	√	• Daylighting discontinuities were observed on the slope face, i.e. they intersected the slope surface within the critical zone which allows blocks to topple outward • The slope angle was slightly steep (50^{o}), which is likely to allow blocks to topple under the influence of gravity
L2	Planar	√	• Dip angles of the sliding planes are greater than the friction angle, i.e. Both 62^{o} and 63^{o} are greater than 30^{o} • The sliding plane (s) daylights in the slope face, i.e. Dip of sliding plane < slope face angle ($62^{o}<72^{o}$; and $63^{o}<72^{o}$)
	Wedge	√	• There was intersection of more than two discontinuity planes within the critical zone., i.e. J_1 &J_3 and J_2 &J_3 • The slope geometry was steep enough to allow the wedge to slide out under gravity, i.e. 72^{o}
	Toppling	√	• The slope angle was very steep (72^{o}), allowing blocks to topple under the influence of gravity • The inclination angles of discontinuity planes (63^{o} & 62^{o}) are greater than the friction angle (30^{o})
L3	Planar	x	• The dip direction of the discontinuity plane deviated by more than 20° from the slope face dip direction; i.e. (280^{o} - 078^{o}) = (202^{o}) >20^{o} • No any sliding plane/critical vector was observed to daylight or intersect in the slope face
	Wedge	x	• The area had only one major discontinuity plane/joint set and also no any critical intersections of joints were observed in the critical zone
	Toppling	√	• Daylighting discontinuities were observed on the slope face, i.e. they intersected the slope surface within the critical zone which allows blocks to topple outward • The slope angle was also steeply inclined (67^{o}), allowing blocks to topple under the influence of gravity
L4	Planar	x	• The dip direction of the discontinuity plane had an angle difference greater than $\pm 20^{o}$ from the slope face direction, hence reduces the likelihood of a planar failure to occur. • No any sliding plane was observed to daylight or intersect in the slope face • No any critical vectors were observed in the critical zone for planar sliding
	Wedge	√	• Several critical intersections were observed within the critical zone • The slope geometry (55^{o}) is also steep enough to allow the wedge to slide out under gravity
	Toppling	√	• A critical joint in favor of flexural toppling was seen to daylight on the slope face within the critical zone, thus may allow blocks to topple outward

Location ID	Failure mode	Possibility of occurrence	Reason (s)
L5	Planar	√	• The sliding plane daylights in the slope face within the critical zone
	Wedge	√	• Several critical intersections were observed within the critical zone • The slope geometry was steep enough to allow the wedge to slide out under gravity, i.e. 65º
	Toppling	√	• Daylighting discontinuities were observed on the slope face, i.e. they intersected the slope surface within the critical zone which allows blocks to topple outward • The slope angle was also steeply inclined (65º), allowing blocks to topple under the influence of gravity
L6	Planar	√	• Some critical vectors (joints) were observed to daylight in the slope face
	Wedge	√	• Two major discontinuity planes (J2 &J3) intersected each other within the critical zone and several other critical intersections were observed • The slope geometry was sufficiently steep (76º) to allow the wedge to slide out under gravity
	Toppling	√	• The slope angle was very steep (76º), allowing blocks to topple under the influence of gravity • Daylighting discontinuities were observed on the slope face, i.e. they intersected the slope surface within the critical zone which is likely to allow blocks to topple outward obliquely
L7	Planar	√	• The sliding plane daylights in the slope face • Dip of the sliding plane was greater than the friction angle, but less than the dip of slope face, (44º>30º) • Dip direction of the discontinuity plane was within the range of 20º of the dip direction of the slope face; i.e. (276º-267º) = 09º
	Wedge	√	• Several critical intersection points were observed to fall within the critical zone, and this indicates that the wedge could potentially slide out of the slope face
	Toppling	√	• Daylighting discontinuities were observed on the slope face, i.e. they intersected the slope surface within the critical zone which is likely to accelerate blocks to topple outward.

5.0 CONCLUSION

This study identified 13 distinct lithological units within the area, each unveiling unique strength characteristics. Most rock units were classified as either poor or fairly strong, corresponding to RMR classes IV and III, respectively. Notably, only the Basement rock formation qualified as a class II rock mass, with an average RMR of 63 and a GSI of 58, suggesting good rock mass quality.

The analysis revealed consistently high variability in RMR values across lithologies, with coefficients of variation (COV) exceeding 10%. This variability indicates significant heterogeneity in rock mass properties, contributing to greater uncertainty in stability assessments and highlighting the need for enhanced geotechnical assessments. In particular, strength parameters such as cohesion exhibited the highest variability (up to 97.4%), while UCS and tensile strength also showed significant variability (COV >30%). The friction angle displayed moderate variability.

Kinematic analysis results further indicated that the area is susceptible to wedge, planar, and toppling failures at varying scales. Several locations exhibited high densities of discontinuities, with failure probabilities exceeding critical thresholds. These findings underscore the importance of implementing slope protection strategies and targeted investigations in areas showing signs of instability, in order to improve safety and operational reliability.

To enhance the reliability of slope stability assessments, the study recommends adoption of advanced analytical techniques such, as finite element modelling and probabilistic methods, which allow for the integration of a wider range of input geotechnical parameters. Furthermore, the current deployment of Slope Stability Radar in monitoring pit slopes at COP F&D should be maintained and strategically expanded to multiple pit locations for real-time monitoring and early detection of slope movement, thereby supporting proactive risk management in mine operations.

Acknowledgement

The authors gratefully acknowledge Konkola Copper Mine Plc (Nchanga Open Pit) for providing access to data utilized in this study. Special appreciation is extended to the geotechnical team at Nchanga Open Pit—Eng. Amory Mumba, Eng. Shoma Syamusana, Mr. Emmanuel Ng'ambi, Mr. Asheo Simwaba, and Mr. Yaled Kaunda—for their invaluable support and assistance during the data collection phase.

References

Abramson, L. W., Lee, T. S., Sharma, S., & Boyce, G. M. (2002). Slope Stability and Stabilization Methods, Second Edition. John Wiley & Sons.

Ahmed, A., Besa, B., Krishna, R., & Umar, S. (2018). Development of Risk Management Guide Lines for Slope Stability Problem at Nchanga Open Pit (NOP) Mine, Zambia. International Journal of Recent Engineering Research and Development (IJRERD) Www.Ijrerd.Com ||, 03, 33–39. www.ijrerd.com

Aladejare, A. E., & Akeju, V. O. (2020). Design and Sensitivity Analysis of Rock Slope Using Monte Carlo Simulation. Geotechnical and Geological Engineering, 38(1), 573–585. https://doi.org/10.1007/s10706-019-01048-z

Alzo'ubi, A. K. (2016). Rock Slopes Processes and Recommended Methods for Analysis. International Journal of GEOMATE, Vol. 11, Issue 25, pp. 2520-2527.

Awang, H., Salmanfarsi, A. F., Aminudin, M. S., & Ali, M. I. (2021). Stability of weathered cut slope by using kinematic analysis. IOP Conference Series: Earth and Environmental Science, 682(1). https://doi.org/10.1088/1755-1315/682/1/012018

Barton, N., Lien, R., & Lunde, J. (1974). Engineering classification of rock masses for the design of tunnel support. Rock Mechanics Felsmechanik Mécanique Des Roches, 6(4), 189–236. https://doi.org/10.1007/BF01239496/METRICS

Bieniawski, Z. (1989). Engineering rock mass classifications: A complete manual for engineers and geologists in mining, civil, and petroleum engineering (New York: John Wiley & Sons).

Chishimba, D & Besa, B. (2023). Development of Tool to Predict Rockburst Potential Using Geotechnical Data: A Case Study of Konkola Mine No.1 Shaft, Zambia; International Journal of Research Publication and Reviews. Volume 4, Issue No. 10, pp 1080-1091. ISSN 2582-7421

Dyke, G. P. (2008). Rock mass characterization: A comparison of the MRMR and IRMR classification systems. The Journal of The Southern African Institute of Mining and Metallurgy.

Dzimunya, N., Besa B., & Nyirenda, R (2023); Prediction of ground vibrations induced by bench blasting using the random forest algorithm; The Journal of the Southern African Institute of Mining and Metallurgy. Volume 123, Issue No. 3, pp 123-132. On-line version ISSN 2411-9717Print version ISSN 2225-6253

Gong, W., Bowa, V. M., Zhao, C., Cheng, Z., & Zhang, L. (2021). Footwall Rock Slope Stability Evaluations at Nchanga Open Pit Mine, Zambia. Geotechnical and Geological Engineering, 39(8), 5753–5765. https://doi.org/10.1007/s10706-021-01864-2

Hoek, E. (1994). Strength of Rock and Rock Masses. ISRM News Journal, 2, 4-16.

Hoek, E., & Bray, J. D. (1981). Rock Slope Engineering (London: Institute of Mining and Metallurgy). https://doi.org/10.1201/9781482267099

Hoek, E., & Brown, E. T. (1997). Practical Estimates of Rock Mass Strength. In Int. J. Rock Mech. Min. Sci (Vol. 34, Issue 8).

Hoek, E., & Brown, E. T. (2019). The Hoek–Brown failure criterion and GSI – 2018 edition. Journal of Rock Mechanics and Geotechnical Engineering, 11(3), 445–463. https://doi.org/10.1016/j.jrmge.2018.08.001

ISSMGE-TC304. (2021). State of The Art Review of Inherent Variability and Uncertainty in Geotechnical Properties and Models. ISSMGE International for Soil Mechanics and Geotechnical Engineering - Technical Committee TC304 'Engineering Practice of Risk Assessment and Management,' 304, 1–220. https://doi.org/10.53243/R0001

Kolapo, P., Oniyide, G. O., Said, K. O., Lawal, A. I., Onifade, M., & Munemo, P. (2022). An Overview of Slope Failure in Mining Operations. Mining, 2(2), 350–384. https://doi.org/10.3390/mining2020019

Laubscher, D. H. (1990). A geomechanics classification system for the rating of rock mass in mine design. 90(10), 257–273.

Mohammed, M. M. (2021). A Review on Slope Monitoring and Application Methods in Open Pit Mining Activities. International Journal of Scientific & Technology Research, 10(02), 2. www.ijstr.org

Ndlovu, S. Z., & Louis Van Rooy, J. (2018). Geotechnical Characterisation and Design Processes for Anisotropic Rock Masses in Open Pits: A Case Study of an Iron Ore Deposit in Orientation Biased Anisotropic Host Rocks.

Norrish, N., & Wyllie, D. C. (1992). Rock Slope Stability Analysis.

Obregon, C., & Mitri, H. (2019). Probabilistic approach for open pit bench slope stability analysis – A mine case study. International Journal of Mining Science and Technology, 29(4), 629–640. https://doi.org/10.1016/j.ijmst.2019.06.017

Oosthuizen, J. (2018). Review of Radar Technologies for Slope Stability in Open-Pit Mines. Southern African Institute of Mining and Metallurgy, 61.

Rafiei Renani, H., Martin, C. D., Varona, P., & Lorig, L. (2019). Stability Analysis of Slopes with Spatially Variable Strength Properties. Rock Mechanics and Rock Engineering, 52(10), 3791–3808. https://doi.org/10.1007/s00603-019-01828-2

Raghuvanshi, T. K. (2019). Plane failure in rock slopes – A review on stability analysis techniques. In Journal of King Saud University - Science (Vol. 31, Issue 1, pp. 101–109). Elsevier B.V. https://doi.org/10.1016/j.jksus.2017.06.004

Rocscience. (2024). Dips User Guide: Tutorials | Tutorials Overview. https://www.rocscience.com/help/dips/tutorials/tutorials-overview

Salmanfarsi, A. F., Awang, H., & Ali, M. I. (2020). Rock mass classification for rock slope stability assessment in Malaysia: A review. IOP Conference Series: Materials Science and Engineering, 712(1). https://doi.org/10.1088/1757-899X/712/1/012035

Salunke, D., Chvan, G., Bartakke, R., & Kothavale, P. (2017). An Overview on Methods for Slope Stability Analysis. www.ijert.org

Sandria, L. A., Budi Indrawan, I. G., & Hendrayana, H. (2023). Rock Mass Characterizations and Kinematic Analysis for Construction Design Method of Diversion Tunnel of Dolok Dam, Central Java. E3S Web of Conferences, 468. https://doi.org/10.1051/e3sconf/202346802005

Simataa, E. (2019). Investigating Slope Stability in Open pit mine- A case study of the Phyllites western wall at Sentinel pit; MSc Thesis.

Singh, B., & Goel, R. K. (2011). Engineering Rock Mass Classification. Butterworth-Heinemann; Elsevier Inc.

Singh, Pradhan, S. P., & Vishal, V. (2011). Stability of slopes in a fire-prone mine in Jharia Coalfield, India. Arabian Journal of Geosciences, 6(2), 419–427. https://doi.org/10.1007/s12517-011-0341-4

Srinivasan, V., Mishra, A. K., Vinoth, S., Kumar, L. A., & Mishra, A. K. (2016). Status and Developments of Slope Monitoring Techniques in Opencast Mines. https://www.researchgate.net/publication/305656162

Verma, D., Thareja, R., Kainthola, A., & Singh, T. N. (2011). Evaluation of Open Pit Mine Slope Stability Analysis. In International Journal of Earth Sciences and Engineering (Vol. 04, Issue 04).

Verma, Sharma, P., Singh, R., & Singh, T. N. (2021). Evaluation of Slope Stability Analysis using Kinematic and Chart Method: A Case Study. Journal of the Geological Society of India, 97(11), 1387–1395. https://doi.org/10.1007/s12594-021-1877-x

Woldeselsassie, E. K., Xiuwen, C., Demissie, D., & Mekonnen, T. (2019). REVIEW ON SLOPE STABILITY ANALYSIS AND EVALUATION. In International Journal of Engineering Applied Sciences and Technology (Vol. 4). http://www.ijeast.com